CONF-860609--12

86009699

DR-1805-8

UCRL- 93421
PREPRINT

MASTER

UCRL--93421

DE86 009699

THERMOMECHANICAL MODELING OF THE SPENT FUEL TEST - CLIMAX

T. R. Butkovich
W. C. Patrick

This paper was prepared for submittal to the
27th U.S. Rock Mechanics Symposium, University
of Alabama, June 23-26, 1986.

February, 1986

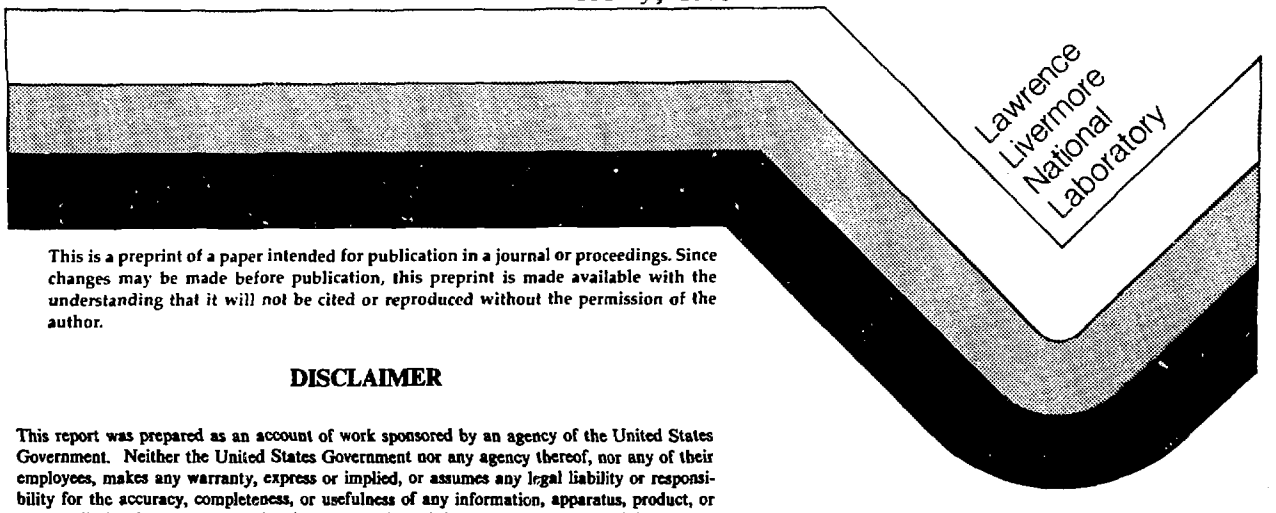

DISCLAIMER

JSW

THERMOMECHANICAL MODELING OF THE SPENT FUEL TEST - CLIMAX

T. B. Butkovich and W. C. Patrick[a]

Lawrence Livermore National Laboratory, P O Box 808, Livermore, CA 94550
[a]J. T. Corporation, Carlsbad, New Mexico

ABSTRACT

The Spent Fuel Test-Climax (SFT-C) was conducted to evaluate the feasibility of retrievable deep geologic storage of commercially generated spent nuclear-reactor fuel assemblies. One of the primary aspects of the test was to measure the thermomechanical response of the rock mass to the extensive heating of a large volume of rock. Instrumentation was emplaced to measure stress changes, relative motion of the rock mass, and tunnel closures during three year of heating from thermally decaying heat sources, followed by a six month cooldown period.

The calculations reported here were performed using the best available input parameters, thermal and mechanical properties, and power levels which were directly measured or inferred from measurements made during the test. This report documents the results of these calculations and compares the results with selected measurements made during heating and cooling of the SFT-C.

INTRODUCTION

A test of retrievable deep geologic storage of spent fuel assemblies from an operating commercial nuclear reactor was recently completed in a granitic intrusive at the U.S. Department of Energy's (DOE) Nevada Test Site. This project, generally referred to as the Spent Fuel Test-Climax (SFT-C), is part of the Nevada Nuclear Waste Storage Investigations, which are managed by the Nevada Operations Office of the DOE. The Lawrence Livermore National Laboratory (LLNL) was responsible for the technical direction of the test.

In addition to evaluating the feasibility of deep geologic storage, the test provided an excellent opportunity to study large scale responses of a granitic rock mass to extensive heating and subsequent cooling to near ambient conditions. Specific test objectives related to the thermomechanical response of the rock mass were to evaluate our ability to numerically model the response of the rock mass to an episode of heating and subsequent cooling.

In order to accomplish this objective, a series of calculations were undertaken using the ADINA structural analysis code (Bathe,1979) and its companion heat flow code ADINAT (Bathe, 1977). These finite element codes were chosen because of their broad acceptance, and their ability to either directly or indirectly treat much of the phenomena of interest in the SFT-C. Of particular importance were the coupling of heat flow and mechanical response, excavation sequencing, arbitrary stress boundary conditions and a provision for simulating ventilation effects. Fault and joint motion were not specifically treated.

TEST DESCRIPTION AND GEOMETRY

Location and Configuration

The SFT-C is located 420 m below the ground surface in the quartz monzonite unit of a two part intrusive known as the Climax stock. At the test level, the rock is about 150 m above the regional water table and is unsaturated but not dry. Wilder and Yow (1984) report four dominant joint sets and three much less prominent sets in the test area. The joint frequencies range from 0.9 to 2.2 joints/m in the test area.

The basic configuration of the test is shown in Figure 1. The three parallel drifts are spaced about 10 m on centers. The dimensions of the two parallel end central canister drift are 3.4 x 3.4 m and 4.6 x 6 m high in cross section respectively.

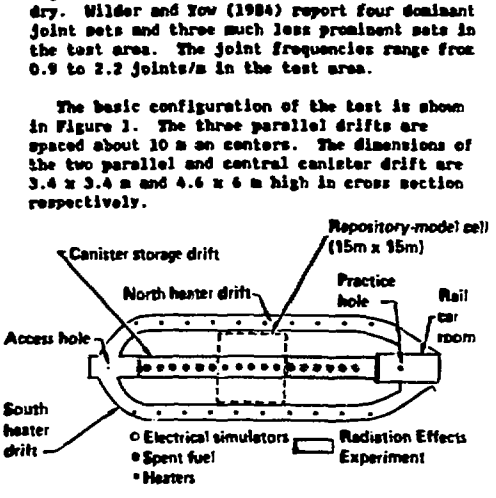

Figure 1. Plan view of SFTC showing locations of spent fuel and related heat sources and thermal phase instrumentation.

Eleven canisters containing single intact spent-fuel assemblies aged about 2.5 years out of core were emplaced in 0.61 m diameter by 6 m deep boreholes drilled in the floor of the central drift. The spent fuel assemblies were interspersed with six electrically heated simulators which were located in boreholes of the same size and geometry. To simulate the thermal field of a large repository, ten auxiliary electrical heaters were located in boreholes spaced 6 m apart in the floor of each of the two side drifts.

Instrumentation

Temperatures, displacements, and stress changes were measured during the three-year heating phase and subsequent six-month cooling phase of the SFT-C. Although the deposition and removal of thermal energy and the concomitant changes in the rock mass temperature constitute the driving force, the displacements and stress changes are of direct concern in this report.

Thermocouples were located throughout the test array to measure the distribution of temperatures during the test. These instruments were mostly concentrated in the regions close to canisters, and were also located to measure temperatures relatively far from the heat sources. Of particular interest here are those thermocouples that were located on or adjacent to instruments which measured displacements or stress changes.

In addition, the characteristics of the ventilation air stream were monitored. The "dry bulb" temperatures and the dewpoints of the inlet and outlet airstreams, together with air flow rates, were used to determine the quantity of energy removed by the ventilation system as a function of time.

Geomechanical instrumentation was located throughout the SFT-C to monitor displacements and stress changes which occurred as the rock mass was initially excavated, heated, and cooled. Multiple borehole extensometers (MPBX) were installed at three orientations in four locations in the pillars between the heater drifts and the canister drift (Fig. 2). Whereas the four horizontally oriented units have three anchor points, the units oriented at 34 and 50 degrees above horizontal each have six anchor points. These units, which are referred to as Mine-by instruments (MBI), were installed to record displacements during the Mineby experiment and were refurbished for continued use during the heating and cooling phases of the test. Subsequent to excavation, 14 four-anchor MPBX units were installed in the floor of the canister drift to measure displacements within the rock mass.

Sixteen orthogonal sets of convergence wire extensometers (CWE) were installed to measure displacements within the drifts. These units measured the relative displacements between the roof and the floor and between opposing walls of the drifts. Each CWE was outfitted to permit parallel tape extensometer measurements to be made.

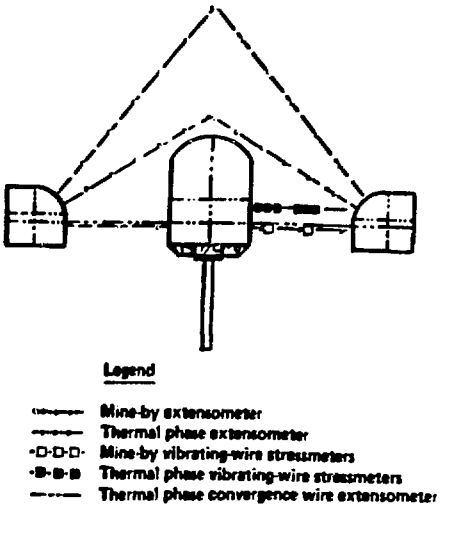

Fig. 2. Cross section showing locations of various instruments in SFT-C.

Changes in the state of stress were monitored at selected locations using IRAD vibrating wire stressmeters. A total of 18 units were installed as rosettes of three, one metre radially outward from each of two spent-fuel assemblies, and at pillar center and 0.7 m in from the canister drift at each of two locations in the north pillar.

A number of the geomechanical instruments experienced malfunctions during the heated phase of the SFT-C. As a result, not all instruments provided continuous data records. The most critical data losses were from the vibrating wire stressmeters.

Energy Deposition and Removal

The power history of the spent fuel, developed by Schmittroth et al. (1980) was adjusted to bring it into better agreement with calorimetry data obtained early in the test. The power history of the electrical simulators was adjusted to the power levels which closely matches the decay curve of the spent fuel.

The spent-fuel assemblies were emplaced and the simulators were energized during a six week period beginning April 18, 1980 and ending May 28, 1980. Likewise, at the end of the heating phase of the test they were retrieved or de-energized as appropriate between March 3, 1983 and April 6, 1983. Because we modeled the facility as a infinite length array using a unit cell approach, these heat sources could not be treated individually in the calculations. Instead, the calculation began to deposit energy at a time corresponding to the insertion of the center spent-fuel assembly (May 8, 1980), and stops when this

assembly was removed (March 24, 1983). All times are based on the spent fuel age in years out of core (YOC). The spent fuel was 2.46 YOC at the start of testing.

The power levels of the auxiliary heaters are shown in Table 1. The power levels of these sources increased as the test progressed. The power increase closely approximates the thermal pulse which is generated by the interaction of many parallel rows of heat sources in a large repository. Since the auxiliary heaters were energized and de-energized simultaneously, the timing of their energy deposition is treated explicitly in the thermomechanical calculations.

Table 1. Auxiliary heater power history.

Date of Change	Power (Watts)	Comments
May 8, 1980	0.	Start of test
June 27, 1980	1850.	Too high
July 2, 1980	925.	Target
December 18, 1980	1250.	Target
February 19, 1982	925.	Too low
March 1, 1982	1400.	Compensating value
April 8, 1982	1350.	Target

The removal of energy from the SFT-C was carefully monitored. Since it was not our goal to evaluate our ability to model removal of energy by the ventilation air stream, we used the measured energy removal rate as a heat sink in our ADINAT calculations. This allowed a better level of agreement between measured and calculated rock temperatures and hence, limited the influence of discrepancies between measured and calculated rock temperature on the thermomechanical response of the rock mass.

HEAT TRANSFER CALCULATIONS AND COMPARISONS WITH DATA

The thermal calculations were carried out with the ADINAT finite element code which is compatible with the ADINA displacement and stress analysis code. ADINAT produces nodal point thermal histories that drive the thermomechanical ADINA calculations.

Correctly modeling heat transfer in the SFT-C requires a heat transfer code with conduction, radiation, and ventilation capabilities. In addition to conductive heat flow through the rock mass, radiative heat transfer occurs between floor, walls, and roof of the drifts. Furthermore, heat is removed by the ventilation air stream passing through the drifts. However, the present version of ADINAT allows radiative heat transfer only from the external boundary of the calculational mesh, and heat transfer to the ventilation air is not directly modeled.

Butkovich and Montan (1980) devised a method that enables ADINAT to model internal radiative heat transport and ventilation. Radiation was modeled by assigning a high value of thermal conductivity and a low mass density to the material which constitutes the openings. To simulate ventilation, we first connected all side nodes in each drift to a central node. This node was then connected to an outside point whose temperature was fixed. A temperature dependent convective heat transfer coefficient controls heat transfer between this outside point and the central node.

The goal of the ADINAT thermal calculation was to produce the correct temperature change with which the thermomechanical calculation would be driven. Therefore, the convection coefficient which controls the rate of removal of heat by the ventilation air stream was varied until good agreement between measured and calculated temperatures was obtained.

Since there is approximate symmetry with respect to the vertical center line through the spent-fuel drift, only half of the planar cross section shown in Fig. 2 was modeled. In constructing the finite element mesh, we made provision for an element group 0.5-m wide surrounding the excavations so that a region around each opening which was damaged by explosives in the mining process could be assigned different properties than the rest of the rock mass. With the exception of degenerated 4-node elements used for the material removed in the excavation, all of the elements consisted of eight nodes.

Table 2 shows the thermal properties of the Climax stock quartz monzonite used in the ADINAT calculations. The power input to the spent fuel canisters and electrical simulators is that shown in Fig. 3 as the solid curve.

Table 2. Thermal properties of Climax stock Quartz Monzonite used in thermal calculation.

Heat capacity[a]	930 J/kg-K
Thermal conductivity	
0°C	3.1679 W/m-K
27	3.1104
477	2.1104
Thermal expansion coefficient[b]	
0°C	10. x 10^{-6}/K
23	10.
40	8.9
80	7.4
125	8.0
175	9.6
225	12.7

[a]Derived from diffusivity measurements
[b]Heard, H., (1979), values based on measurements at effective pressure at 13.8 MPa.

The convection coefficients (which control heat transfer out of the mesh) were varied until a good fit to all of the temperature data measured throughout the entire heating and cooling

portions of the test was produced. Figure 4 shows a typical temperature-time curve comparing measured and calculated results. The nodal point temperatures throughout the mesh at the start of the calculation was 23.5° C. The measured temperatures were within about one degree of this average value.

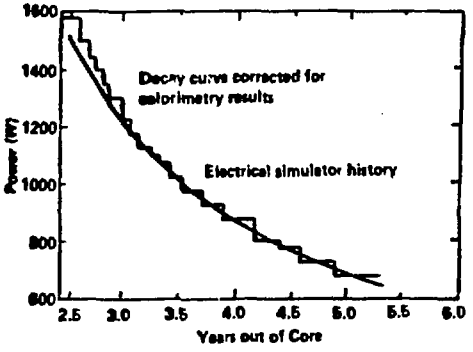

Fig. 3. Power input to spent fuel canisters and electrical simulator.

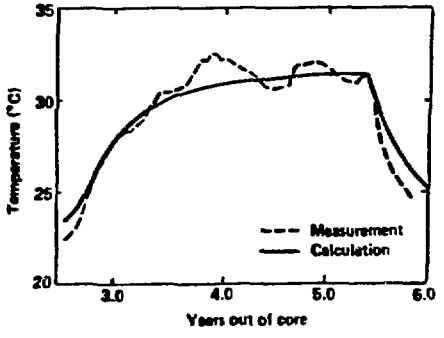

Fig. 4. Typical temperature-time curve comparing measured and calculated results.

Fig. 5 shows an example of a comparison between the measured and calculated values of temperature change since the start of the test for 30 locations above and below the openings at station 2+83, near the center of the test facility at a time 5.0 YOC. If the calculation and measurements agreed exactly, all the points would fall on the line with slope = 1 and y-intercept = 0. Also shown are the slope (A1) and y-intercept (A0) of the best fit straight line and the root-mean-square errors (RM). In all cases, we see R^2 (RR) values of at least 0.98 and root-mean-square errors of less than 1°C. These compare favorably with the IRM special limits of error for thermocouples (1.1°C) and with the individual calibrations. This is an exceptionally good level of agreement when one considers that the positions of the temperature measurement points are not coincident with nodal points in the finite element mesh for which the calculated temperatures are shown. Around the rib where the elements are smaller, the nodal points are within 0.25 m of a measurement point. For regions away from the openings where the mesh is more coarse, the nodal points may be as much as 1.0 m away from associated measurement points.

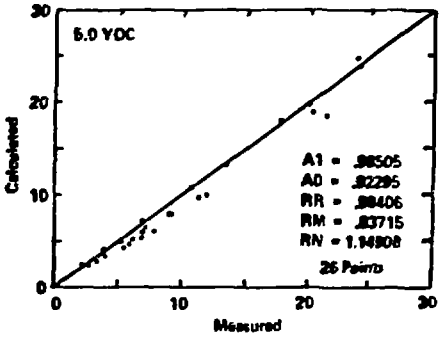

Fig. 5. Comparison between measured and calculated values of temperature changes since start of test at station 2+83 at 5 YOC.

THERMOMECHANICAL RESPONSE CALCULATIONS AND COMPARISON WITH DATA

General Considerations and Input Data

After the heating phase of SFT-C was completed, Creveling et al. (1984) performed an extensive suite of stress measurements using two independent techniques in boreholes up to 30 m in length. The measurements exhibited a high degree of spatial variability both in magnitude and in orientation.

In situ deformability data for the SFT-C were initially developed by Heuze et al. (1981). Later, Patrick, Yow, and Axelrod (1985) completed deformation modulus measurements following the heated phase of the test. Their analyses show that: the mean deformation modulus was 37.7 GPa, about 40% higher; while their mean modulus of faulted, sheared or intensely jointed rock agreed with the earlier estimate.

Upon examination of the available in situ stress and deformation moduli data, it seemed unreasonable to do calculations for all the possible combinations within the range of measurements. Furthermore, it was not possible to model the variability directly. Instead, three thermomechanical calculations were made, one using the in situ values estimated by Heuze et al. (1981), the second based on best estimates of in-situ values of Patrick, Yow and Axelrod (1985), and the third with mesh loadings based on the extreme of the post test in-situ stress measurements. Each of these calculations used the same nodal point temperature histories obtained with ADINAT, and temperature dependent thermal expansion coeffi-

cients shown in Table 2. The thermal expansion coefficients used were taken from Heard (1979). He measured the expansion coefficients on samples of EPT-C quartz monzonite at confining pressures of 0, 13.6 and 27.8 MPa. The intermediate set of values were used as more representative, based on measured in-situ stress at test level. The values of input parameters for the three calculations were as shown in Table 3.

Table 3. Elastic properties and mesh loading used for three thermomechanical calculations.

	CALCULATION NUMBER		
	1	2	3
Moduli (GPa)			
Intact	27	38	38
Damaged	13	19	19
Poisson's Ratio			
Intact	0.25	0.25	0.25
Damaged	0.35	0.35	0.35
Loading (MPa)			
Vertical*	6.21	6.21	12.60
Hor./Vert.	1.2	1.2	0.98

*Vertical mesh loading based on in-situ stresses measured at mid-rib.

Comparisons Between Calculations and Data

Results of the three calculations are shown for stress changes, tunnel closure, and relative displacements within the rock mass around the openings. When comparisons with measurements are shown, stress differences between two times are used; tunnel closures are adjusted to a calculation as of the start of the measurement period (several weeks after the start of heating) and are compared with the calculation from then until the end of the test; and relative displacement differences are compared at selected times during the test.

Stress Changes

The three points for which stress vs time results are shown coincide with the positions of stress gauges. Figure 6 shows the calculated vertical stress vs time for a point midheight in the pillar, 3 m from the heater drift. Figure 7 shows similar results for a point in the floor of the canister drift at midpoint elevation of the center spent-fuel canister, and 1.18 m radially outward from its centerline.

Comparing the results of these calculations, we see moderate differences between calculations 1 and 2 where the mesh loading is the same but the deformation moduli differ by about 40%. Larger differences occur in calculation 3 where the mesh loading is about 80% greater than in the other calculations.

As a result of failure of the IRAD vibrating-wire stress gauges early in the test, it is impossible to compare calculations with data during most of the heating phase of the test. These failures occurred when the gauge housings leaked, causing corrosion of the wire. The instruments were redesigned with better seals and re-installed shortly before the spent fuel was removed. Stress measurements at three locations, two of which are cited above, were available from this time through the cooldown period.

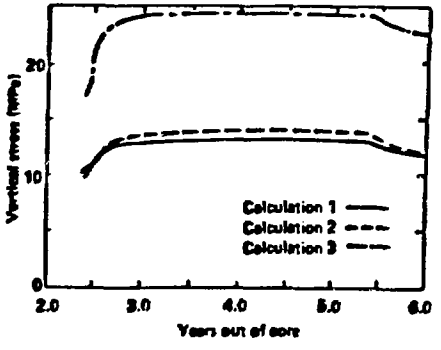

Fig. 6. Calculated in-plane vertical stress vs time for a point at mid-height in pillar, 3 m from heater drift.

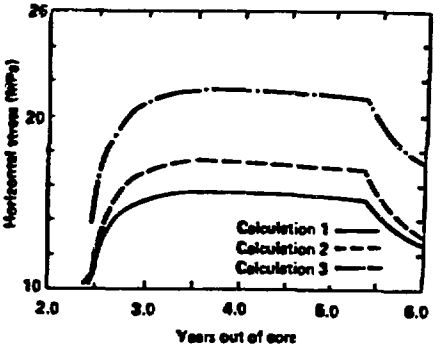

Fig. 7. Calculated in-plane vertical stress vs time for a point at mid-height elevation of spent fuel canister, 1.18 m from its axis.

To make these comparisons, the results from the stress-gauge rosettes were used to calculate the secondary principal stresses for times of interest. From these, the horizontal stress component in the plane of the calculation was determined. Vertical in-plane stress values were measured directly with stressmeters in the horizontal boreholes which are located in the ribs at mid-height at two stations.

Table 4 shows comparisons of measured stress differences at the two stations for each gauge position with those calculated for the position between 5.35 YDC and 5.85 YDC for each location. In comparing the measurements and calculations, the accuracy of the measurements must be considered. Patrick, Becker, and Scarafiotti (1984) report post-test calibrations for the stressmeters which show errors in the range of 250% of the gauge readings. The measured and calculated changes in stress agree within the uncertainties of the measurements.

Table 4. Comparison of measured and calculated stress changes which occurred during cooldown period.

Station #	Measured MPa	Calculated MPa #1	#2	#3
Horizontal - 1.18 m from mid-point elevation of spent fuel				
3+58	3.5	2.4	3.4	3.4
2+98	3.3			
Vertical - mid-height in rib 0.7 m from canister drift				
2+85	2.1	1.0	1.3	1.4
3+47	8.9			
Vertical - mid-height in rib at mid-rib				
2+28	0.6	1.1	1.4	1.4
3+47	0.3			

Tunnel Closure

Measurements of drift deformations were made routinely since the emplacement of the spent fuel. Both horizontal and vertical measurements were taken at five locations along the heater drifts and at six locations along the canister drift. Two types of instrumentation were used: convergence wire extensometers which were monitored automatically, and a manually operated tape extensometer with which measurements were made periodically, typically once each month. The tape extensometer measurements were initiated six weeks after the emplacement of the spent fuel.

Figures 8 and 9 show an example of calculated horizontal and vertical spent fuel drift closures for each calculation. The results from these calculations show the complexity of the effects of varying in situ stresses and moduli. At all locations, calculation 2 provides the smallest tunnel closures because it used both the lower in situ stress and higher moduli. Although calculation 1 shows the greatest horizontal convergence in the canister drift, there is essentially no difference between calculations 1 and 3 in the heater drift, even though the in situ stresses are markedly higher for calculation 3. It also provides the greatest vertical tunnel closure in both the canister and heater drifts.

Measurements from five locations in the canister drift, five in the north heater drift, and four in the south heater drift may be compared with calculated displacements. Temperature corrected tape extensometer measurements from redundant measurements and different operators were arithmetically averaged to produce a single closure curves for the horizontal and vertical directions in each drift. The measurement variations range to a maximum of 20.2 mm about the mean. However, these variations have not been correlated with local properties and geologic structures and hence are taken to be random in this analysis.

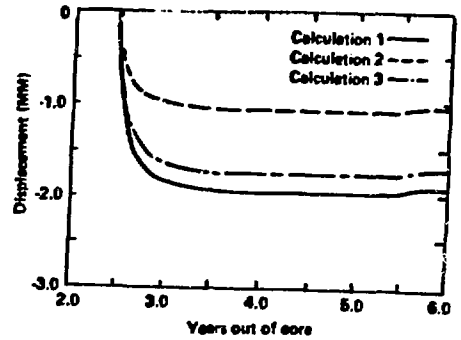

Fig. 8. Calculated horizontal closure of the Spent Fuel Drift.

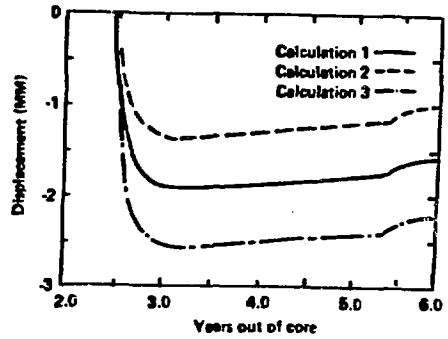

Fig. 9. Calculated vertical closure of the Spent Fuel Drift.

The calculations show that as much as 2/3 of the maximum closure took place before the first tape extensometer measurements were made. As a result, it was necessary to add the amount of calculated closure to the averaged measured values to facilitate a comparison. For this, Calculation #2 was chosen since average values of measured modulus were used and mesh loading was based on best estimates of in situ stress.

Figure 10 shows an example of a comparison for horizontal canister drift closure.

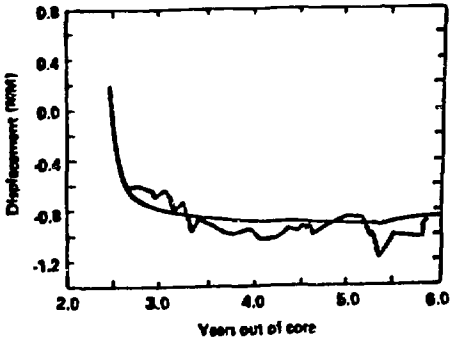

Fig. 10. An example of a comparison between calculation and measurements of drift closure.

Although the averaged measurements appear somewhat erratic because of the marginally acceptable resolution of the instrument (about 0.025 mm), the calculations and the measurements track each other quite well. First, the measured and calculated tunnel closures are similar in form. For the measurements showing closure during the entire heating period, the calculational results also show this effect. Where the measurements show closure followed by dilation, the calculation shows this effect as well. Second, the magnitudes of closures provided by Calculation 2 appear to be in good agreement with the measured responses.

When the difference between measurements and calculation is being considered, the reader should keep in mind that the fractional difference should be based on the total closure. Measurements began toward the end of a period when the closure rates are quite high. Therefore a small change from the assumption that both curves are connected at the time of the first measurement can make the agreement between measurement and calculation change dramatically.

Relative Displacements of the Rock Mass

Comparisons may also be made between temperature corrected measurements within the rock mass and calculations. The finite element mesh nodal points that were selected for these comparisons were near or intersected by the positions of the horizontal and inclined borehole rod extensometers. Since the calculations provide horizontal and vertical displacement components it was necessary to trigonometrically project these components onto the 34° and 50° inclined positions which correspond to the extensometers. These results were compared with the appropriate measured displacement.

Corrections were made for the thermal expansion of the rods. These corrections were, in every case, a factor of two or more larger than the recorded displacements. This is because the coefficient of expansion of the steel rods from which the rod extensometers were made is similar to that of the rock. That is, both rock and instruments expand nearly the same amount under a given temperature change. As a result, the measured displacements contain a large component from the expansion of the instrument, a small component reflecting the difference between rock and instrument expansion, and a possible third component due to inelastic rock response.

Once again, no data were available for the early part of the test so it was necessary to make all comparisons relative to a spent-fuel age of 3.0 TOC, approximately six months after emplacement of the spent fuel.

The relative displacement data are summarized for ease of analysis in Figs. 11. More 230 measured and calculated displacements are plotted against each other. A line fit through the points provides some basic measures of how well the data compare to the calculations. Calculation 2 is nominally better than the other calculations by all three measures. While the R^2 is rather low (RR = 0.574), it is somewhat better than the 0.517 and 0.524 of Calculations 1 and 3, respectively. In addition, the root-mean-square error of the data with respect to the least-squares fit is about 5 mm less for Calculation 2. The relatively small R^2 and large RMS error can be explained, in large part, by errors in the instrumentation. In situ calibrations indicated errors of about 10 ± 60 mm (at one σ) with errors for individual instruments ranging ± 0.25 mm (Patrick, Hector, and Scarafiotti, 1984). Therefore, the data and calculations cannot agree any better than this.

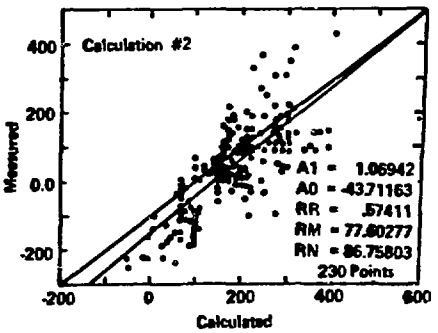

Fig. 11. Comparisons of measured and calculated relative displacements with results from calculation 2.

Within these limitations, we conclude that Calculation 2 provided the best agreement with the data. This calculation used average rock-mass moduli, a half-metre thick explosively damaged zone around each opening, and the average in situ stress magnitudes which resulted in a horizontal-to-vertical stress ratio of 1.2.

SUMMARY AND REMARKS

The Spent Fuel Test-Climax caused extensive heating of a large volume of granitic rock. Although other tests of this type have been conducted, this was the first opportunity to evaluate the ability of a finite-element code such as ADINA to calculate thermomechanical responses of rock on this large a scale. Calculations were performed using the best available thermomechanical properties and in situ stresses for the rock surrounding the mined openings which comprised the SFT-C. The ADINA calculations all used an isotropic thermoelastic model with temperature dependent thermal expansion coefficients.

In general, the measured and calculated displacements agree within the accuracy of the instrumentation. This is tempered by the fact that measurements were not obtained at early times when rates of displacements and stress changes were very high. Furthermore, intrinsic limitations of transducer accuracies make highly precise comparisons between data and calculations impossible.

It appears then, that the rock mass where measurements were made behaves thermoelastically. However, a companion paper by Wilder (1986) notes significantly larger non-recoverable deformations towards the ends of the SFT-C drifts, where faults and shear zones occur, while the central region where the reported measurements were taken has ubiquitous jointing. We are led to conclude that the rock at SFT-C with ubiquitous jointing behaves elastically, with largely recoverable deformations on cooling. In the regions where shear zones and faults occur, the deformations are larger and only partially recoverable.

ACKNOWLEDGMENTS

Prepared by Nevada Waste Storage Investigations (NNWSI) Project participants as part of the Civilian Radioactive Waste Management Program. The NNWSI Project is managed by the Waste Management Project Office of the U.S. Department of Energy, Nevada Operations Office. NNWSI Project work is sponsored by the Office of Geologic Repositories of the DOE Office of Civilian Radioactive Waste Management.

Work performed under the auspices of the U.S. Department of Energy by Lawrence Livermore National Laboratory under contract W-7405-ENG-48

REFERENCES

1. Bathe, K.J. (1977), ADINAT, A Finite Element Program for Automatic Dynamic Incremental Analysis of Temperature, Massachusetts Institute of Technology, Cambridge, MA, Rept. No. 82448-5.

2. Bathe, K.J. (1978), ADINA, A Finite Element Program for Automatic Dynamic Incremental Nonlinear Analysis, Massachusetts Institute of Technology, Cambridge, MA, Rept. No. 72448-1.

3. Butkovich, T.R., and Montan, D.N. (1980), A Method for Calculating Internal Radiation and Ventilation with the ADINAT Heat-Flow code, Lawrence Livermore National Laboratory, Livermore, Cal. UCRL-52918.

4. Creveling, J.B., Shuri, F.S., Foster, K.N., and Mills, S.V.,(1984), In Situ Stress Measurements at the Spent Fuel Test-Climax Facility, LLNL Contractor Report UCRL-15628, Submitted by Foundations Sciences Inc., Portland, OR.

5. Heard, H. C. (1979), Thermal Expansion and Inferred Permeability of Climax Quartz Monzonite to 300 K and 27.6 MPa, Lawrence Livermore National Laboratory, Livermore, Cal. UCRL 83697.

6. House, F., Patrick, W.C., de la Cruz, R.V., and Voss, C.F. (1981), In Situ Geomechanics Climax Granite, NTS, Lawrence Livermore National Laboratory, Livermore, Cal. UCRL 53076.

7. Patrick, W.C., Hector, N.L., and Scarafiotti, J.J., (1984), Instrumentation Report #3: Performance and Reliability of Instrumentation Deployed for the Spent Fuel Test-Climax, Lawrence Livermore National Laboratory, Livermore, Cal. UCRL 53657.

8. Patrick, W.C, Yow, J.L. Jr.,and Axelrod, M.C., (1986) Measurement of In Situ Deformability with the EX Borehole Jack, SFT-C, Nevada Test Site, Lawrence Livermore Laboratory, Livermore, Ca. UCRL in preparation.

9. Schmittroth, F., Healy, C.J. and Krogness, J.C. (1980), A Comparison of Measured and Calculated Decay Heat for Spent Fuel near 2.5 Years Cooling Time, Hanford Engineering Development Laboratory, Richland, WA, HEDL-TC-1759.

10. Wilder, D.G. and Yow, J.L. Jr. (1984) Structural Geology Report, Spent Fuel Test-Climax, Nevada Test Site, Lawrence Livermore National Laboratory Livermore, CA, UCRL 53381.

11. Wilder, D.G. (1986) "Inelastic Deformations of Fault and Shear Zones in Granitic Rock", Lawrence Livermore National Laboratory, Livermore, CA, UCRL-93422.

LEGIBILITY NOTICE

A major purpose of the Technical Information Center is to provide the broadest possible dissemination of information contained in DOE's Research and Development Reports to business, industry, the academic community, and federal, state, and local governments. Non-DOE originated information is also disseminated by the Technical Information Center to support ongoing DOE programs.

Although large portions of this report are not reproducible, it is being made available only in paper copy form to facilitate the availability of those parts of the document which are legible. Copies may be obtained from the National Technical Information Service. Authorized recipients may obtain a copy directly from the Department of Energy's Technical Information Center.